A Time-dependent Heliospheric Model Driven by Empirical Boundary Conditions

SH23D-2699

Tae K. Kim[1], Charles "Nick" Arge[1,2], and Nikolai V. Pogorelov[1,3]

[1]Center for Space Plasma and Aeronomic Research, University of Alabama in Huntsville, Huntsville, AL, USA

[2]NASA Goddard Space Flight Center, Greenbelt, MD, USA

[3]Department of Space Science, University of Alabama in Huntsville, Huntsville, AL, USA

1. Introduction

Solar Wind

- A stream of charged particles originating from the Sun
- A medium in which the solar magnetic field and energy propagate outward
- Primary driver of space weather

Heliosphere

- A "bubble-like" structure formed by the pressure balance between the solar wind and the local interstellar medium (LISM) as illustrated in Figure 1
- Size and shape largely affected by fluctuations in the solar wind parameters
- Heliopause: the boundary between the solar wind and the LISM plasma
- Heliosheath: the region characterized by compressed, turbulent, subsonic plasma flow
- Termination shock: the boundary across which the supersonic solar wind slows down to subsonic speeds

Sun-Earth

- Earth is in the inner heliosphere, where the solar wind is the predominant component of interplanetary plasma
- Solar wind modeling is a critical component of space weather study

The Heliosphere

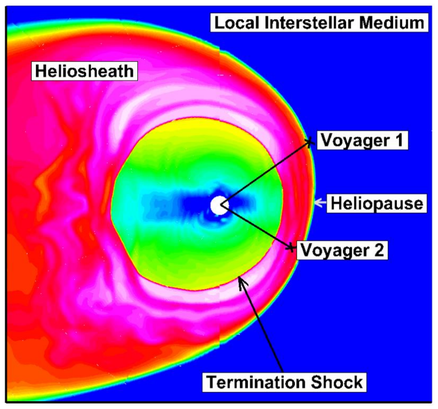

Figure 1. The heliosphere and the Voyager spacecraft trajectories

2. Modeling Software

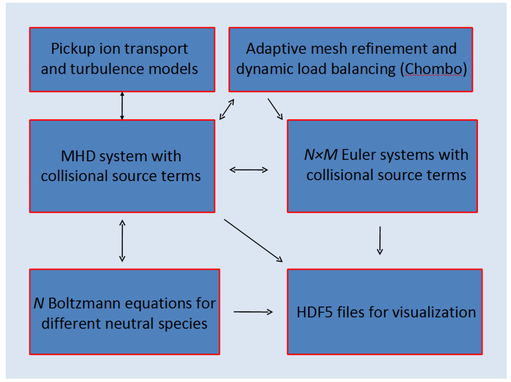

Figure 2. Block diagram of MS-FLUKSS (Pogorelov et al. 2011)

- **Multi-Scale Fluid-Kinetic Simulation Suite (MS-FLUKSS)**
  - A package of numerical codes designed to model the heliosphere in multiple scales and high resolution
  - Adaptive mesh refinement based on Chombo architecture (Colella et al. 2007)
  - MHD treatment for solar wind / LISM plasma and fluid treatment for neutral hydrogen atoms (1, 2, 4, or 5 fluids) (Pogorelov et al. 2008)
  - MHD treatment for solar wind / LISM plasma and kinetic treatment for neutral hydrogen atoms (Pogorelov et al. 2008; Borovikov et al. 2008; Heerikhuisen et al. 2008)
  - Turbulence model for supersonic solar wind (Pogorelov et al. 2012; Kryukov et al. 2012)
  - Time-dependent boundary conditions from in situ measurements of the solar wind (e.g., Pogorelov et al. 2013; Kryukov et al. 2012; Kim et al. 2016, 2017)
  - Realistic 3-D time-dependent boundary conditions from remote-sensing observations of the solar wind (e.g., Kim et al. 2014a; 2014b)

3. Simulation Results

Boundary Conditions from the Wang-Sheeley-Arge (WSA) model

- WSA: semi-empirical coronal model for the ambient solar wind (Arge et al. 2003, 2004)
- Potential field source surface (PFSS) model + current sheet model
- Input from synoptic magnetograms or Air Force Data Assimilative Photospheric Flux Transport (ADAPT) model at the Sun's surface (Arge et al. 2010, 2012, 2013)
- Solar wind speed estimated as a function of the flux expansion factor and the distance to the nearest coronal hole boundary (Arge et al. 2003, 2005)
- Coupled with heliospheric MHD models such as ENLIL and MAS as part of CORHEL

MS-FLUKSS Heliospheric 3-D MHD Model

- Single-fluid ideal MHD solar wind flow from 0.1 to 1.5 AU
- Input from ADAPT-WSA model output (interplanetary magnetic field and solar wind speed) at 0.1 AU
- **Density and temperature at the inner boundary estimated using either ad hoc assumptions (labeled as Model 1) or empirical correlations (labeled as Model 2)**

Estimation of Density and Temperature at 0.1 AU

- Ad hoc prescription assuming momentum and thermal pressure balance:
  e.g., WSA-ENLIL v2.7: $nV^2 = 300 \times 650^2$ (constant kinetic energy) and $nT = 300 \times 0.8$ (constant pressure) at 21.5 R_S, where n is number density in cm^{-3}, V is radial velocity in km/s, and T is temperature in MK.
- Density-speed and temperature-speed correlations from Ulysses data up to 2009 (Pogorelov et al. 2013):

Solar Cycle 23

- Slow wind ($v_R < 450$ km/s)

$$T = 10^5 R^{-0.68} [0.80 + 0.0217 \times (v_R R^{-0.048} - 388)],$$

$$n = R^{-1.93} [6.37 - 0.0292 \times (v_R R^{-0.048} - 388)],$$

- Fast wind ($v_R > 450$ km/s)

$$T = 10^5 R^{-0.95} [2.21 + 0.000233 \times (v_R R^{-0.06} - 668)],$$

$$n = R^{-1.93} [2.27 - 0.0085 \times (v_R R^{-0.06} - 668)],$$

where T, n, v_R, and R represent the proton temperature (K), number density (cm^{-3}), radial velocity (km/s), and the heliocentric distance (AU), respectively.

- Density-speed and temperature-speed correlations from OMNI data (Elliott et al. 2016):

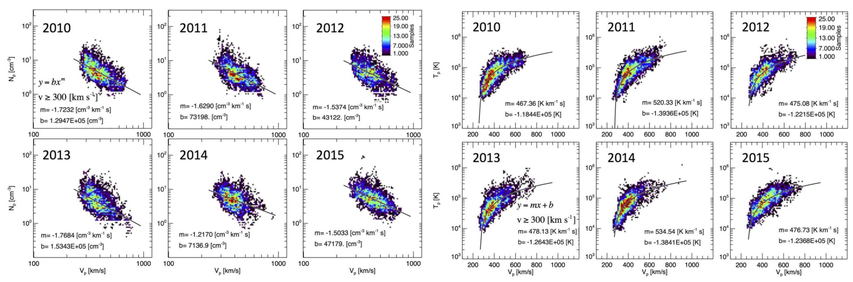

Figure 3. Density–speed distribution plots (top two rows) and temperature-speed plots (bottom two rows) spanning from 2010 to 2015. After removing the ICMEs, the remaining hourly OMNI T_p–V_p observations are placed in 2D bins, and color coded by the number of points per bin. The fits are performed to all the hourly samples with the ICMEs removed, but without any binning. The black curves show linear fits over most of the energy range, and the fitting procedure is the same as those in Elliott et al. (2012), where the measurements with speeds from 330 to 850 km/s were fit. Taken from Elliot et al. (2016).

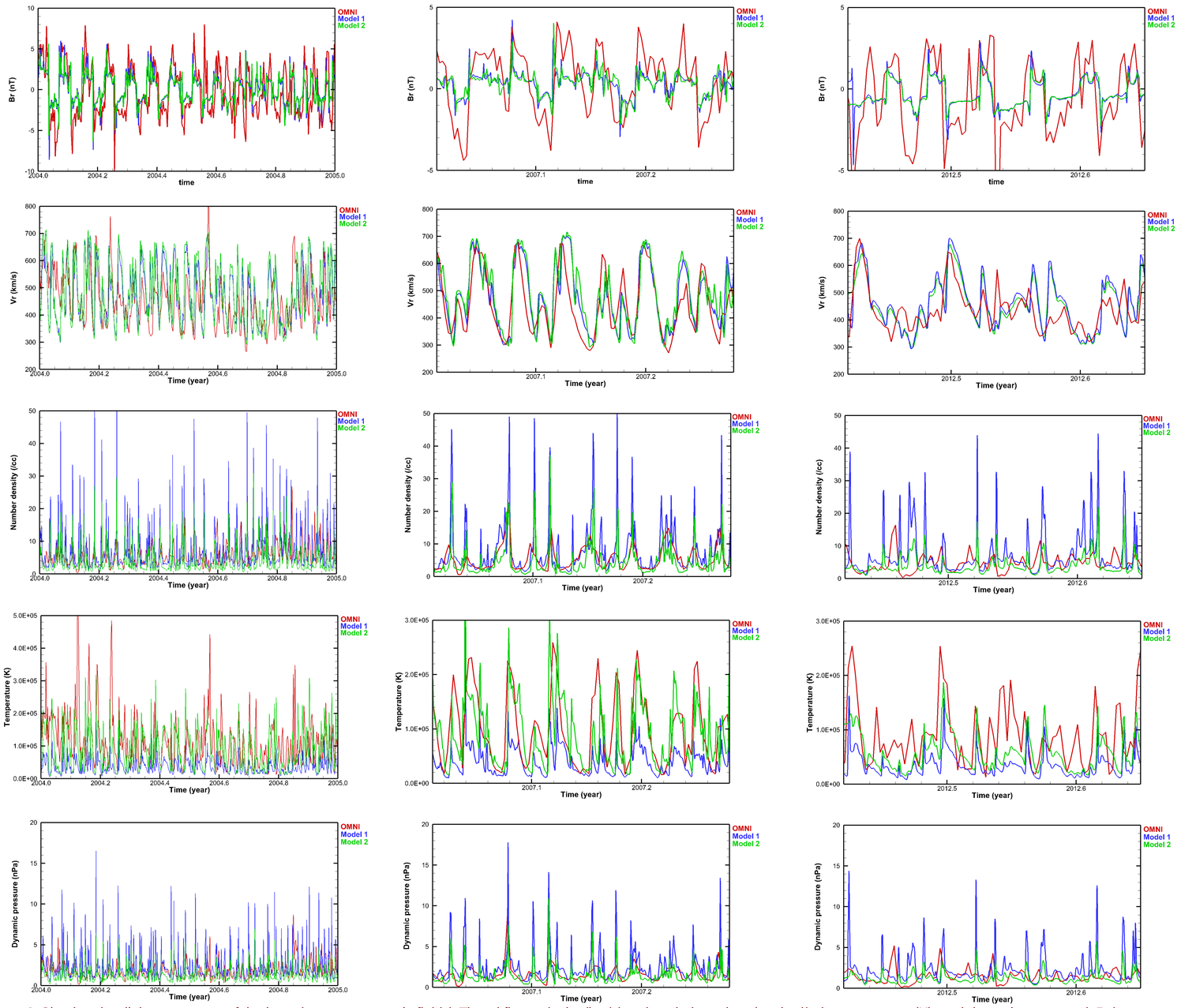

Figure 4. Simulated radial components of the interplanetary magnetic field (nT) and flow velocity (km/s), solar wind number density (/cc), temperature (K), and dynamic pressure (nPa) compared with OMNI data at Earth for three different periods

4. Summary and Discussions

- MS-FLUKSS 3-D heliospheric model coupled with ADAPT-WSA coronal model
- Simulation of time-dependent flow of the ambient solar wind from 0.1 to 1.5 AU
- Magnetic field and velocity at 0.1 AU from ADAPT-WSA model
- Density and temperature at 0.1 AU estimated using ad hoc assumptions (Model 1) or empirical correlations (Model 2)
- Models output compared with OMNI data at Earth for three different periods: 2004, 2007, and 2012
- Magnetic field and velocity nearly identical for Model 1 and 2
- Density and temperature for Model 2 agree more favorably with OMNI data
- Ad hoc assumptions of density and velocity may be tweaked to possibly improve Model 1 (e.g., WSA-ENLIL v2.8)
- No tweaking required for the Model 2 approach, which should be considered as an alternate, more consistent approach

References

Arge et al. 2003, *AIP Conference Series*, 679, 190
Arge et al. 2004, *Journal of Atmospheric and Solar-Terrestrial Physics*, 66, 1295
Arge et al. 2005, *ASP Conference Series*, 346, 371
Arge et al. 2010, *AIP Conference Series*, 1216, 343
Arge et al. 2011, *ASP Conference Series*, 444, 99
Arge et al. 2013, *AIP Conference Series*, 1539, 11
Borovikov et al. 2008, *ASP Conference Series*, 385, 197
Colella et al. 2007, *Journal of Physics: Conference Series*, 78, 012013
Elliott et al. 2012, *Science* 341, 1489
Elliott et al. 2016, *Astrophysical Journal*, 809, 121
Heerikhuisen et al. 2008, *ASP Conference Series*, 385, 204
Kim et al. 2014a, *ASP Conference Series*, 484, 91
Kim et al. 2014b, *Journal of Geophysical Research*, 119, 7981-7997
Kim et al. 2016, *Astrophysical Journal*, 832, 72
Kim et al. 2017, *Astrophysical Journal Letters*, 843, L32
Kryukov et al. 2012, *AIP Conference Series*, 1436, 48
Pogorelov et al. 2008, *ASP Conference Series*, 385, 180
Pogorelov et al. 2011, *ASP Conference Series*, 444, 130
Pogorelov et al. 2012, *AIP Conference Series*, 1436, 321
Pogorelov et al. 2013, *Astrophysical Journal*, 772, 2

Acknowledgments

This work is supported by the NSF PRAC award OCI-1144120 and related computer resources from the Blue Waters sustained-petascale computing project. Supercomputer time allocations were also provided on SGI Pleiades by NASA High-End Computing Program award SMD-15-5860 and on Stampede and Comet by NSF XSEDE project MCA07S033. T.K.K. and N.V.P. acknowledge support from the NSF SHINE project AGS-1358386, SAO subcontract SV4-84017, and NASA contract NNX14AF41G. The authors acknowledge use of the SPDF COHOWeb database for OMNI data.